Identification of Dynamic Vehicular Axle Loads: Theory and Simulations

LU DENG

C. S. CAI

Department of Civil and Environmental Engineering, Louisiana State University, Baton Rouge, LA 70803, USA (CSCAI@LSU.EDU)

Abstract: This paper presents a new method of identifying dynamic vehicular axle loads by directly using bridge measurements. To demonstrate how the proposed methodology works out, vehicle-bridge coupling equations are first established for numerical simulations. The developed vehicle-bridge coupled system contains only the modal properties of the bridge and the physical parameters of the vehicle. Using the superposition principle and influence surface concept, the dynamic interaction forces (i.e. the dynamic axle loads) can then be identified from the measured bridge responses. A series of simulations are carried out in which the effects of various factors such as bridge inertia force, measurement station, vehicle speed, traveling route, number of vehicles, road surface condition, and noise level have been investigated. The identified results show that the proposed method is able to identify dynamic axle loads with good accuracy, which can serve as a basis for dynamic bridge-weigh-in-motion. This paper also serves as a theoretical base for the companion paper in which the proposed method is applied to identify the dynamic axle loads of a real truck on an existing bridge.

1. INTRODUCTION

Dynamic-load-induced bridge responses can be much more significant than static responses, causing more damage to bridges. Cebon (1987) concluded that the dynamic axle loads may increase the road surface damage by a factor of two to four compared to the static axle loads. While impact factors are used in bridge designs generally to quantify the dynamic effect of axle loads (AASHTO 2002, 2004), impact factors are largely affected by site-specific information, such as the roughness of bridge deck surface and bridge dynamic characteristics. Site-specific information of vehicle dynamic effects is very desirable for performance evaluation of existing bridges and even in guiding designs of new bridges. However, it is difficult to directly measure the dynamic axle loads because they are moving and varying with time.

Traditionally, the moving vehicular loads are either measured directly from an instrumented vehicle (Heywood, 1996) or computed from the models of the bridge deck and vehi-

cle (Green and Cebon, 1994; Yang and Yau, 1997; Henchi et al., 1998). The first method is very expensive and difficult to implement, and the results obtained are subject to bias since the measurement is limited only to the instrumented vehicles, while the second method is subject to modeling errors. To obtain site-specific information of vehicle weight, weigh-in-motion systems have also been developed in the last few decades (Peters, 1984), but they usually measure only static axle loads, requiring a smooth road surface or slow vehicle movement to eliminate the dynamic effects (Leming and Stalford, 2002). Therefore, it would be beneficial if the dynamic axle forces of routine traffic vehicles could be identified from measured bridge responses, since such information is very valuable for bridge engineers.

In recent years, many techniques of identifying moving loads on bridges have been proposed. A comprehensive literature review of recent research on the identification of moving loads was reported by Yu and Chan (2007). Bridge responses such as strain, displacement, acceleration, and bending moment have all been used in the identification process (O'Conner and Chan, 1988; Law et al., 1997; Chan et al., 1999; Law et al., 1999; Law et al., 2001; Yu and Chan, 2003; Chan and Ashebo, 2006; Pinkaew, 2006; Pinkaew and Asnachinda, 2007). O'Conner and Chan (1988) proposed the Interpretive Method I (IMI), which is able to identify dynamic axle forces of multi-axle systems. In their numerical study the bridge is modeled as an assembly of lumped masses interconnected by massless elastic beam elements. Later, the time domain method (TDM) (Law et al., 1997) and the frequency-time domain method (FTDM) (Law et al., 1999) were proposed, both of which are based on the exact analytical solution and system identification theory.

Another method named Interpretative Method II (IMII), which is similar to the IMI, was also introduced by Chan et al. (1999). Comparative studies of these four methods were conducted by Chan et al. (2000). Regularization methods have also been introduced to solve an ill-conditioned problem, which has been found in most moving force identification methods (Law et al., 2001; Pinkaew, 2006).

In most previous works on moving force identifications, the bridge is modeled as a beam, either a simply supported beam (Law et al., 1997, 1999, 2001) or a multi-span continuous beam (Zhu and Law, 2002; Chan and Ashebo, 2006). While it is a good approach to demonstrate the concept, the beam-model-based methodology would become unrealistic when applied to 3-D real bridges. Although the orthotropic plate model, which is better than the beam model when modeling more complicated bridges such as slab bridges, was also proposed to model the bridge deck by some researchers (Zhu and Law, 2003; Law et al., 2007), few of the previous works have dealt with real bridge structures.

Moreover, only in a few cases has the vehicle-bridge coupling effect been taken into consideration during the axle load identification process (Chan et al., 1999; Pinkaew, 2006). Even in the vehicle-bridge coupled model used by Pinkaew (2006), the bridge is modeled as an oversimplified uniform simply-supported beam.

Obviously, the previous beam-model-based studies are more conceptual than practical, and most of them are limited to numerical simulations. In this paper a new moving force identification method is presented using the superposition principle and influence surface concept to deal with actual bridge structures and the vehicle-bridge coupled situation. A series of case studies are carried out in which the effects of various factors such as bridge inertia force, measurement station, vehicle speed, traveling route, number of vehicles, road surface condition, and noise level are numerically investigated.
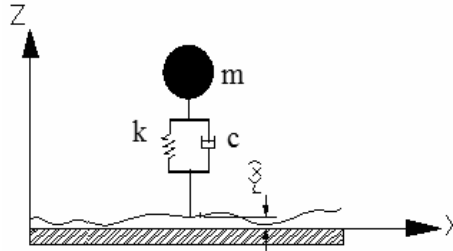
Figure 1. A SDOF vehicle model.

The identified results show that the proposed method is able to identify the dynamic axle loads with good accuracy. This paper also serves as a theoretical base for the companion paper (Deng and Cai, 2008) in which the proposed method is applied to identify the dynamic axle loads of a real truck on an existing bridge. It is noted that the vehicle-bridge interaction analysis, while used in the present numerical simulations, is not required when the measured bridge responses are actually used in field applications as demonstrated in the companion paper.

2. VEHICLE-BRIDGE COUPLED SYSTEM

2.1. Vehicle Model

A review of the different vehicle models used in the literature was reported by Yu and Chan (2007). For the purpose of simplicity of presentation, in the present study a single-degree-of-freedom (SDOF) system consisting of a mass, spring, and damper (Figure 1) was used to establish the vehicle-bridge coupling equations and to demonstrate how the proposed method works out. The SDOF system has proved adequate to simulate the interaction between a single wheel (or vehicle) and the bridge deck (Chatterjee et al., 1994; Yang et al., 2000; Bilello et al., 2004). It should be noted that the methodology can similarly be applied to a full-scale multi-degrees-of-freedom (MDOF) vehicle model, which is usually represented by a combination of rigid bodies connected by a series of springs and damping devices (Huang and Wang, 1992; Zhang et al., 2006; Shi et al., 2008). As demonstrated in the companion paper (Deng and Cai, 2008), a full-scale MDOF vehicle model (Shi, 2006) is used to simulate a real truck whose axle loads are successfully identified from measurements using the proposed methodology. For both the SDOF and MDOF models, the contact between the vehicle and bridge deck is assumed to be a point contact.

The equation of motion of a SDOF vehicle can be written as below according to Newton's Second Law:

$$M_v \cdot \ddot{d}_v = -F_G + F_{v-b} \tag{1}$$

where M_v is the mass of the vehicle; $\ddot{d}_v$ is the acceleration of the vehicle in the vertical direction; F_G is the gravity force of the vehicle; and F_{v-b} is the interaction force between the vehicle and bridge deck, which can be calculated as:

$$F_{v-b} = -K_v \cdot \Delta_L - C_v \dot{\Delta}_L \qquad (2)$$

where K_v and C_v are the coefficients of the vehicle spring and damper, respectively; and Δ_L is the deformation of the vehicle spring.

For the case when n vehicles are traveling on a bridge at the same time, the equations of motion for n vehicles can be written in a matrix form as:

$$[M_v]\{\ddot{d}_v\} = -\{F_G\} + \{F_{v-b}\} \qquad (3)$$

where $[M_v]$ is the diagonal mass matrix for n vehicles; $\{\ddot{d}_v\}$ is the acceleration vector in the vertical direction for n vehicles; and $\{F_G\}$ and $\{F_{v-b}\}$ are the gravity force vector and the interaction force vector for n vehicles, respectively.

2.2. Bridge Model

The equation of motion for a bridge can be written as follows:

$$[M_b]\{\ddot{d}_b\} + [C_b]\{\dot{d}_b\} + [K_b]\{d_b\} = \{F_b\} \qquad (4)$$

where $[M_b]$, $[C_b]$, and $[K_b]$ are the mass, damping, and stiffness matrices of the bridge, respectively; $\{d_b\}$ is the displacement vector for all DOFs of the bridge; $\{\dot{d}_b\}$ and $\{\ddot{d}_b\}$ are the first and second derivative of $\{d_b\}$ with respect to time, respectively; and $\{F_b\}$ is a vector containing all external forces acting on the bridge.

With the modal superposition technique, the displacement vector of the bridge $\{d_b\}$ in equation (4) can be expressed as:

$$\{d_b\} = \begin{bmatrix} \{\Phi_1\} & \{\Phi_2\} & \cdots & \{\Phi_m\} \end{bmatrix} \begin{Bmatrix} \xi_1 & \xi_2 & \cdots & \xi_m \end{Bmatrix}^T = [\Phi_b]\{\xi_b\} \qquad (5)$$

where m is the total number of modes used for the bridge under consideration; $\{\Phi_i\}$ and ξ_i are the ith mode shape of the bridge and the ith generalized modal coordinate, respectively. Each mode shape is normalized such that $\{\Phi_i\}^T[M_b]\{\Phi_i\} = 1$ and $\{\Phi_i\}^T[K_b]\{\Phi_i\} = \omega_i^2$.

In this study the damping matrix $[C_b]$ in equation (4) is assumed to be equal to $2\omega_i\eta_i[M_b]$, where η_i is the percentage of the critical damping for the ith mode of the bridge. equation (4) can now be rewritten as:

$$[I]\{\ddot{\xi}_b\} + 2[\omega_i\eta_i I]\{\dot{\xi}_b\} + [\omega_i^2 I]\{\xi_b\} = [\Phi_b]^T\{F_b\} \qquad (6)$$

where

$$
[\omega_i \eta_i I] =
\begin{bmatrix}
\omega_1 \eta_1 & & & & \\
& \ddots & & & \\
& & \omega_i \eta_i & & \\
& & & \ddots & \\
& & & & \omega_m \eta_m
\end{bmatrix}
, \quad
[\omega_i^2 I] =
\begin{bmatrix}
\omega_1^2 & & & & \\
& \ddots & & & \\
& & \omega_i^2 & & \\
& & & \ddots & \\
& & & & \omega_m^2
\end{bmatrix}
,
$$

for the convenience of derivation, and $[I]$ = unit matrix.

2.3. Road Surface Condition

The road surface condition is an important factor that affects the dynamic responses of both the bridge and vehicles. A road surface profile is usually assumed to be a zero-mean stationary Gaussian random process and can be generated through an inverse Fourier transformation based on a power spectral density (PSD) function (Dodds and Robson, 1973) as:

$$
r(X) = \sum_{k=1}^{N} \sqrt{2\varphi(n_k)\Delta n} \cos(2\pi n_k X + \theta_k) \tag{7}
$$

where θ_k is the random phase angle uniformly distributed from 0 to 2π; $\varphi()$ is the PSD function (m³/cycle/m) for the road surface elevation; and n_k is the wave number (cycle/m). In the present study, the following PSD function (Huang and Wang, 1992) was used:

$$
\varphi(n) = \varphi(n_0) \left(\frac{n}{n_0} \right)^{-2} \quad (n_1 < n < n_2) \tag{8}
$$

where n is the spatial frequency (cycle/m); n_0 is the discontinuity frequency of $1/2\pi$ (cycle/m); $\varphi(n_0)$ is the roughness coefficient (m³/cycle) whose value is chosen depending on the road condition; and n_1 and n_2 are the lower and upper cut-off frequencies, respectively.

The International Organization for Standardization (ISO, 1995) has proposed a road roughness classification index from A (very good) to H (very poor) according to different values of $\varphi(n_0)$. In this paper the classification of road roughness based on the ISO (1995) was used.

2.4. Assembling the Vehicle-bridge Coupled System

Vehicles traveling on a bridge are connected to the bridge via contact points. The wheel-road interaction forces acting on the bridge $\{F_{b-v}\}$ and the interaction forces acting on the vehicles $\{F_{v-b}\}$ are actually action and reaction forces existing at the contact points. In terms of finite element modeling, these interaction forces may not apply right at any element node. Therefore, the interaction forces need to be transformed into equivalent nodal forces $\{F_b^{eq}\}$ in the finite element analysis. According to the virtual work principle and the concept of shape function it is easy to understand that the work done by the actual force directly acting

on one element F and by the equivalent nodal forces $\{F_e^{eq}\}$ should be equal; therefore the following relationship holds:

$$\{F_e^{eq}\} = [N_e]^T \cdot F \tag{9}$$

where $[N_e]$ is a one row shape function matrix of the element in contact, and superscript T stands for the transpose of matrix.

To be consistent with the size of the force vector in the analysis of the full bridge, equation (9) can be expanded to a full force vector form as below:

$$\{F_b^{eq}\} = [N_b]^T \cdot F \tag{10}$$

where $\{F_b^{eq}\}$ is an expanded vector of $\{F_e^{eq}\}$ with the dimension equal to the total number of DOFs of the bridge. For the purpose of convenience, we name $[N_b]$ as the shape function of the bridge. For two interaction forces acting upon different positions of the same bridge, the corresponding $[N_b]$ for the two forces would be different though the element shape function $[N_e]$ may be the same, because the non-zero terms in the two force vectors are interaction force location dependent.

In a vehicle-bridge system, the relationship among the vertical displacement of vehicle body d_v, bridge deflection at the contact point $d_{b\_contact}$, deformation of vehicle spring Δ_L, and road surface profile $r(x)$ can be expressed by the following equation:

$$\Delta_L = d_v - d_{b\_contact} - r(x). \tag{11}$$

The first derivative of equation (11) can then be obtained as follows:

$$\dot{\Delta}_L = \dot{d}_v - \dot{d}_{b\_contact} - \dot{r}(x) \tag{12}$$

where $\dot{d}_v$ is the velocity of the vehicle body in the vertical direction; $\dot{r}(x) = \frac{dr(x)}{dx} \frac{dx}{dt} = \frac{dr(x)}{dx} V(t)$, where $V(t)$ is the vehicle traveling velocity (either variable or constant); and $d_{b\_contact}$, according to the definition of the shape function of the bridge in equation (10), can be expressed as follows:

$$d_{b\_contact} = [N_b] \cdot \{d_b\}. \tag{13}$$

In a situation when n vehicles are present on a bridge, by substituting equations (11), (12), and (13) into equation (2) the interaction force acting on the ith vehicle is obtained as follows:

$$
\begin{aligned}
F_{v-b}^i &= -K_v^i \cdot \Delta_L^i - C_v^i \cdot \dot{\Delta}_L^i \\
&= -K_v^i \cdot \left(d_v^i - [N_b^i]\{d_b\} - r(x)^i \right) - C_v^i \\
&\quad \cdot \left(\dot{d}_v^i - \frac{d[N_b^i]}{dx} \frac{dx}{dt} \{d_b\} - [N_b^i]\{\dot{d}_b\} - \frac{dr(x)^i}{dx} V^i(t) \right) \tag{14}
\end{aligned}
$$

where $\left[N_b^i\right]$ is the shape function of the bridge for the interaction force between the ith vehicle and the bridge. The n interaction forces acting on the n vehicles can be expressed in a vector form as follows:

$$\{F_{v-b}\} = \begin{bmatrix} F_{v-b}^1 & F_{v-b}^2 & \cdots & F_{v-b}^n \end{bmatrix}^T$$

$$= -[K_v]\{d_v\} + \left[K_{v-b}\right]\{d_b\} + \{F_{v-r}\} - [C_v]\{\dot{d_v}\}$$

$$+ \left[K_{v-cb}\right]\{d_b\} + \left[C_{v-b}\right]\{\dot{d_b}\} + \{F_{v-cr}\} \qquad (15)$$

where $[K_v]$ and $[C_v]$ are the diagonal stiffness and damping matrices for the n vehicles, respectively; $\{d_b\}$ and $\{\dot{d_b}\}$ have the same definitions as in equation (4); and $\left[K_{v-b}\right]$, $\{F_{v-r}\}$, $\left[K_{v-cb}\right]$, $\left[C_{v-b}\right]$, and $\{F_{v-cr}\}$ are defined respectively as:

$$\left[K_{v-b}\right] = [K_v] \cdot \begin{bmatrix} \left[N_b^1\right]^T & \left[N_b^2\right]^T & \cdots & \left[N_b^n\right]^T \end{bmatrix}^T ;$$

$$\{F_{v-r}\} = [K_v] \cdot \begin{bmatrix} r(x)^1 & r(x)^2 & \cdots & r(x)^n \end{bmatrix}^T ;$$

$$\left[K_{v-cb}\right] = [C_v] \frac{d \begin{bmatrix} V^1(t) \cdot \left[N_b^1\right]^T & V^2(t) \cdot \left[N_b^2\right]^T & \cdots & V^n(t) \cdot \left[N_b^n\right]^T \end{bmatrix}^T}{dx} ;$$

$$\left[C_{v-b}\right] = [C_v] \cdot \begin{bmatrix} \left[N_b^1\right]^T & \left[N_b^2\right]^T & \cdots & \left[N_b^n\right]^T \end{bmatrix}^T ;$$

$$\{F_{v-cr}\} = [C_v] \cdot \begin{bmatrix} \frac{dr(x)^1}{dx} V^1(t) & \frac{dr(x)^2}{dx} V^2(t) & \cdots & \frac{dr(x)^n}{dx} V^n(t) \end{bmatrix}^T .$$

As discussed earlier, the interaction forces acting on the bridge, $\{F_{b-v}\}$, are the reaction forces of that acting on the vehicles, $\{F_{v-b}\}$. Therefore, the following relationship holds:

$$\{F_{b-v}\} = -\{F_{v-b}\} . \qquad (16)$$

Substituting equations (14) and (16) into equation (10), the transformed equivalent nodal forces due to the N interaction forces can be obtained as follows:

$$\{F_b^{eq}\} = \sum_{i=1}^{n} \left[N_b^i\right]^T \cdot (-F_{v-b}^i)$$

$$= \sum_{i=1}^{n} \left[N_b^i\right]^T \cdot \left(K_v^i \cdot \left(d_v^i - \left[N_b^i\right]\{d_b\} - r(x)^i \right) + C_v^i \right.$$

$$\cdot \left(\overset{\bullet}{d}_v^i - \frac{d\left[N_b^i\right]}{dx}\frac{dx}{dt}\{d_b\} - \left[N_b^i\right]\{\overset{\bullet}{d}_b\} - \frac{dr(x)^i}{dx}V^i(t) \right)$$

$$= \left[K_{b-v}\right]\{d_v\} - \left[K_{b-vb}\right]\{d_b\} - \{F_{b-r}\} + \left[C_{b-v}\right]\{\overset{\bullet}{d}_v\}$$

$$- \left[K_{b-cb}\right]\{d_b\} - \left[C_{b-b}\right]\{\overset{\bullet}{d}_b\} - \{F_{b-cr}\} \tag{17}$$

where $\left[K_{b-v}\right], \left[K_{b-vb}\right], \{F_{b-r}\}, \left[C_{b-v}\right], \left[K_{b-cb}\right], \left[C_{b-b}\right]$, and $\{F_{b-cr}\}$ are defined as follows:

$$\left[K_{b-v}\right] = \left\{ \left[N_b^1\right]^T \cdot K_v^1 \quad \left[N_b^2\right]^T \cdot K_v^2 \quad \cdots \left[N_b^n\right]^T \cdot K_v^n \right\};$$

$$\left[K_{b-vb}\right] = \sum_{i=1}^{n}\left[N_b^i\right]^T \cdot K_v^i \cdot \left[N_b^i\right];$$

$$\{F_{b-r}\} = \sum_{i=1}^{n}\left[N_b^i\right]^T \cdot K_v^i \cdot r(x)^i;$$

$$\left[C_{b-v}\right] = \left\{ \left[N_b^1\right]^T \cdot C_v^1 \quad \left[N_b^2\right]^T \cdot C_v^2 \quad \cdots \left[N_b^n\right]^T \cdot C_v^n \right\};$$

$$\left[K_{b-cb}\right] = \sum_{i=1}^{n}\left[N_b^i\right]^T \cdot C_v^i \cdot \frac{d\left[N_b^i\right]}{dx}V^i(t);$$

$$\left[C_{b-b}\right] = \sum_{i=1}^{n}\left[N_b^i\right]^T \cdot C_v^i \cdot \left[N_b^i\right];$$

$$\{F_{b-cr}\} = \sum_{i=1}^{n}\left[N_b^i\right]^T \cdot C_v^i \cdot \left(\frac{dr(x)^i}{dx}V^i(t) \right).$$

Substituting equation (15) into equation (3), we have the following:

$$[M_v]\{\overset{\bullet\bullet}{d}_v\} = -\{F_G\} - [K_v]\{d_v\} + \left[K_{v-b}\right]\{d_b\} + \{F_{v-r}\}$$

$$- [C_v]\{\overset{\bullet}{d}_v\} + \left[K_{v-cb}\right]\{d_b\} + \left[C_{v-b}\right]\{\overset{\bullet}{d}_b\} + \{F_{v-cr}\}. \tag{18}$$

Since $\left\{F_b^{eq}\right\}$ in equation (17) is actually the equivalent force vector of the external force vector $\{F_b\}$ in equation (4), after substituting equation (17) into equation (4), the following can be obtained:

$$[M_b]\{\ddot{d}_b\} + [C_b]\{\dot{d}_b\} + [K_b]\{d_b\}$$

$$= \left[K_{b-v}\right]\{d_v\} - \left[K_{b-vb}\right]\{d_b\} - \{F_{b-r}\} + \left[C_{b-v}\right]\{\dot{d}_v\}$$

$$- \left[K_{b-cb}\right]\{d_b\} - \left[C_{b-b}\right]\{\dot{d}_b\} - \{F_{b-cr}\}. \tag{19}$$

Equations (18) and (19) can be combined and rewritten in matrix form as below:

$$\begin{bmatrix} M_b & \\ & M_v \end{bmatrix} \begin{Bmatrix} \ddot{d}_b \\ \ddot{d}_v \end{Bmatrix} + \begin{bmatrix} C_b + C_{b-b} & -C_{b-v} \\ -C_{v-b} & C_v \end{bmatrix} \begin{Bmatrix} \dot{d}_b \\ \dot{d}_v \end{Bmatrix}$$

$$+ \begin{bmatrix} K_b + K_{b-vb} + K_{b-cb} & -K_{b-v} \\ -K_{v-b} - K_{v-cb} & K_v \end{bmatrix} \begin{Bmatrix} d_b \\ d_v \end{Bmatrix} = \begin{Bmatrix} -F_{b-r} - F_{b-cr} \\ F_{v-r} + F_{v-cr} - F_G \end{Bmatrix}. \tag{20}$$

Compared to equations (3) and (4), there are additional terms, C_{b-b}, C_{b-v}, C_{v-b}, K_{b-vb}, K_{b-cb}, K_{b-v}, K_{v-b}, K_{v-cb}, F_{b-r}, F_{b-cr}, F_{v-r}, and F_{v-cr} in equation (20), which are resulted due to the coupling effect between the bridge and vehicles. When a vehicle travels on the bridge, the position of the contact point changes with time, which means the road roughness $r(x)$ at the contact point and the shape function $[N_b]$ are both time-dependent terms, indicating that all the additional terms in equation (20) are time-dependent terms.

Using equation (6), equation (20) can be further rewritten as follows:

$$\begin{bmatrix} I & \\ & M_v \end{bmatrix} \begin{Bmatrix} \ddot{\xi}_b \\ \ddot{d}_v \end{Bmatrix} + \begin{bmatrix} 2\omega_i \eta_i I + \Phi_b^T C_{b-b} \Phi_b & -\Phi_b^T C_{b-v} \\ -C_{v-b} \Phi_b & C_v^N \end{bmatrix} \begin{Bmatrix} \dot{\xi}_b \\ \dot{d}_v \end{Bmatrix}$$

$$+ \begin{bmatrix} \omega_i^2 I + \Phi_b^T (K_{b-vb} + K_{b-cb}) \Phi_b & -\Phi_b^T K_{b-v} \\ -(K_{v-b} + K_{v-cb}) \Phi_b & K_v \end{bmatrix} \begin{Bmatrix} \xi_b \\ d_v \end{Bmatrix}$$

$$= \begin{Bmatrix} -\Phi_b^T (F_{b-r} + F_{b-cr}) \\ F_{v-r} + F_{v-cr} - F_G \end{Bmatrix} \tag{21}$$

where the vehicle-bridge coupled system contains only the modal properties of the bridge and the physical parameters of the vehicles.

Based on the above methodology, a MATLAB program named BIRDS-BVI (laboratory of Bridge Innovative Research and Dynamics of Structures – Bridge Vehicle Interaction) was developed to assemble the motion equations of the vehicle-bridge coupled system and to solve the coupling equations. The modal information can be obtained using any commercialized finite element package, such as ANSYS.

Equation (21), once assembled, can be solved by the Rounge-Kutta method in time domain in MATLAB environment. At each time step, the sub-stiffness and sub-damping matrices in equation (21) are first determined, among which the time-dependent terms are determined by the position of vehicles. The interaction forces at the contact points (in the

right-hand side of equation (21)) are then calculated using equation (15). It should be noted that if any interaction force turns out to be negative, which means the corresponding vehicle leaves the road surface, it should be set to zero and the solution is repeated at this step. In such a way this model can account for the situation when vehicles lose contact with the road surface. With all information available, variables of both bridge and vehicle in equation (21) can be solved in a one-step fashion without iteration between the bridge and vehicle displacements.

The solutions to the coupling equations include the displacement of the bridge in the modal coordinate as well as the physical displacement of the vehicles at each time step.

Also can be obtained are the interaction forces, velocity and acceleration of the bridge in the modal coordinate, and physical velocity and acceleration of the vehicles at each time step. The physical displacement of each node on the bridge can then be transformed from the modal coordinate using equation (5). The strain at any node i of the bridge in the longitudinal direction can also be approximately calculated using the expression below:

$$\epsilon(i, t) = \frac{\delta L}{L} = \frac{d_{i+1}(t) + d_{i-1}(t) - 2d_i(t)}{2L} \tag{22}$$

where L represents the distance between two adjacent nodes in the longitudinal direction and $d_{i-1}(t)$, $d_i(t)$, and $d_{i+1}(t)$ denote the displacements of three consecutive nodes in the longitudinal direction respectively. The strain information will be used later for the identification of vehicle axle loads.

3. METHODOLOGY OF AXLE FORCE IDENTIFICATION

As discussed earlier, the vehicle axle loads will eventually be identified with actual bridge measurements. The previous section has developed the methodology of vehicle-bridge interaction from which the dynamic axle loads can be predicted. To show the concept prior to actual applications, this predicted axle load will be treated as "true" value in the present numerical simulations and will be compared with the identified axle loads for conceptual verifications. The identification methodology of axle loads is presented below.

Bridges in service can be reasonably approximated as linear systems; therefore, the superposition principle can be used. For a bridge subjected to n moving axle loads, the magnitude of damping force during routine service is much smaller than other forces and can thus be ignored for axle load identifications, though it is included in the vehicle-bridge simulations. The vehicle-induced response of the bridge, such as the deflection or strain, at a certain point on the bridge can be expressed as:

$$R_{total} = r_{inertia} + \sum_{i=1}^{n} r_i \tag{23}$$

where R_{total} is the total response of the bridge; $r_{inertia}$ is the part caused by the inertia force of bridge vibrations (more details on how to obtain $r_{inertia}$ will be provided in the numerical simulations); and r_i is the response caused by the interaction force from the ith vehicle. It is

noted that no other forces such as wind induced bridge responses are considered here. This expression for the decomposition of the bridge response was also mentioned by Yu and Chan (2007). Using the concept of influence surface (influence line in a 3D format), from equation (23) we can easily obtain the following:

$$\sum_{i=1}^{n} f_i \cdot h_i = R_{total} - r_{inertia} \tag{24}$$

where f_i is the interaction force from the ith vehicle and h_i is the response value on the influence surface at the position of the ith vehicle.

In the case when n forces $(f_1, f_2, \cdots, f_n)$ are to be identified, we need to have at least n set of measurements to solve the n simultaneous equations in a matrix form as follows:

$$[H]_{n \times n} \{F\}_{n \times 1} = \{R\}_{n \times 1} \tag{25}$$

where $[H]$ is the matrix for h_i; $\{F\}$ is the vector for f_i; and $\{R\}$ is the vector of interaction-force-induced response, representing the right hand side of equation (24).

Now the interaction forces between the n vehicles and bridge can be obtained by solving equation (25) using the least-squares method as follows:

$$\{F\}_{n \times 1} = \left([H]_{n \times n}^T \cdot [H]_{n \times n}\right)^{-1} \cdot [H]_{n \times n}^T \cdot \{R\}_{n \times 1} . \tag{26}$$

The solution to equation (26) may be ill-conditioned since the values of the influence surface at the beginning and the end of the bridge are very small. The regularization method developed by Tikhonov (1963) can be used and the corrected solution is obtained as follows:

$$\{F\}_{n \times 1} = \left([H]_{n \times n}^T \cdot [H]_{n \times n} + \lambda I\right)^{-1} \cdot [H]_{n \times n}^T \cdot \{R\}_{n \times 1} \tag{27}$$

where λ is a non-negative regularization parameter and I is the identity matrix.

4. NUMERICAL SIMULATIONS

To study the accuracy and efficiency of the proposed identification method, numerical simulations were carried out and a series of comprehensive case studies were conducted.

The SDOF vehicle model was used in the following simulation study for the purpose of simplicity, and both the deflection and strain histories were used in the identification process. The identification error can be defined as:

$$\text{Identification Error} = \frac{\sum\limits_{i=1}^{J} |F_{iden}(i) - F_{true}(i)|}{\sum\limits_{i=1}^{J} |F_{true}(i)|} \times 100\% \tag{28}$$
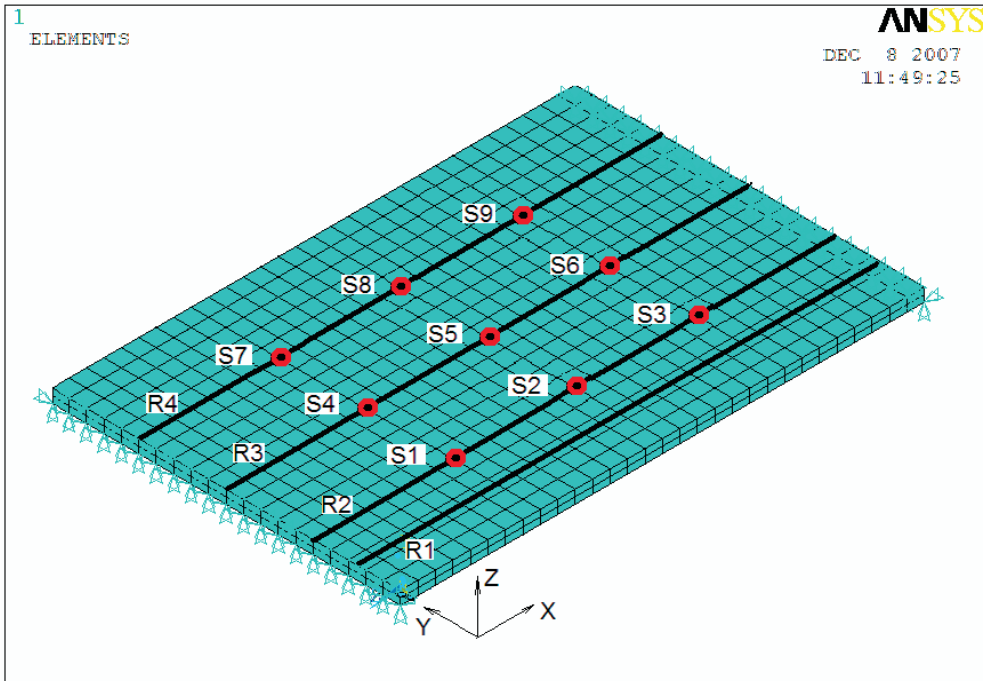
Figure 2. The concrete slab bridge under study.

where $F_{iden}(i)$ and $F_{true}(i)$ are the identified interaction force and the true interaction force, respectively, at the ith step and J is the total number of time steps. The $F_{iden}(i)$ is identified using equation (27); the $F_{true}(i)$ is obtained either with equation (15) by solving the vehicle-bridge coupling equations, or actually measured from the field.

A simply supported concrete slab bridge is used in all case studies for demonstration of the procedure. The bridge has a length of 12 m, a width of 8 m, and a depth of 0.3 m. This bridge is modeled using solid elements (with three translational DOFs for each node) with the ANSYS program (Figure 2). The density, modulus of elasticity, and Poisson's ratio of the concrete are 2300 kg/m³, 210 GPa, and 0.15, respectively. The parameters of all the vehicles used in this study are taken as follows: $m_v = 5 \times 10^3$ kg; $k_v = 1.0 \times 10^6$ N/m; and $c_v = 5.0 \times 10^2$ Ns/m. The speed of the vehicle is set to be 10 m/s in all cases except those studying the effect of different vehicle speeds. The time interval between two time steps is taken as 0.001 s.

In this study a total of 9 measurement stations located at the bottom of the bridge deck are originally selected from the bridge (Figure 2). Because of the symmetry among the 9 measurement stations selected, only 4 of them (S1, S2, S4, and S5) are studied, whose positions are listed in Table 1. Four traveling routes, R1, R2, R3, and R4, are used in the present study, with lateral positions of Y1 = 1m, Y2 = 2 m, Y3 = 4m, and Y4 = 6m, respectively, as indicated in Figure 2.
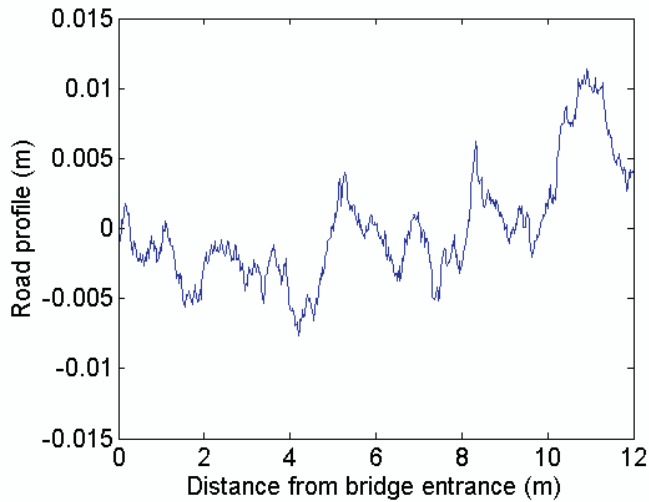
Figure 3. An average-condition road surface profile used in the present study.

Table 1. Positions of measurement stations.

Measurement station	X (m)	Y (m)
S1	3.2	2.0
S2	6.0	2.0
S4	3.2	4.0
S5	6.0	4.0

The same road surface profile (Figure 3), which belongs to an average road surface condition based on the ISO (1995), is used in all case studies except those studying the effect of different road surface conditions. The significance of the effect of bridge inertia force on the identification results is examined first. The effects of different vehicle speeds, traveling routes, number of vehicles, measurement stations, road surface conditions, and levels of noise are also examined. Errors of the identified results for all the case studies are summarized in Table 2 and will be discussed separately later.

4.1. *Effect of Bridge Inertia Force*

While inertia forces are always included in dynamic simulations, their effect on the iden- tified interaction forces was investigated since this effect was usually ignored in the bridge weigh-in-motion practice (Leming and Stalford, 2002). Both the deflection and the strain information from S5 while the vehicle is traveling along R2 were used in this identification process. As discussed earlier, the dynamic response of the bridge, such as the deflection and strain, can be attributed to two causes, the interaction forces from the vehicles traveling on the bridge and the inertia force of the bridge itself, if the small damping force is neglected. Figure 4 shows the decomposition of the deflection and strain into two parts, one caused by

Table 2. Summary of results for errors in various case studies.

Bridge response used		Error (%)	
		Deflection	Strain
Considering bridge inertia force	No	29.69	32.51
	Yes	0.78	10.36
Measurement station	S5	0.78	10.36
	S4	1.40	13.26
	S2	8.53	18.07
	S1	13.95	27.37
Vehicle speed	5 m/s	0.90	10.55
	10 m/s	0.78	10.36
	20 m/s	0.93	10.92
Traveling route	R1	0.24	10.78
	R2	0.78	10.36
	R3	0.78	10.87
Road surface condition	Good	0.76	10.42
	Average	0.78	10.36
	Poor	1.24	10.27
Noise level	5%	2.72	10.63
	10%	5.37	12.22
Two vehicles	1st Vehicle	5.15	20.62
	2nd Vehicle	3.62	17.09

the bridge inertia force, and the other by the interaction force from the vehicle. As shown in the figure, the bridge response due to the inertia force itself is significant compared with that caused directly by the interaction force from the vehicle. If the inertia force is ignored, a 30% level of error is shown in Table 2 for this particular example.

The portion of bridge response caused by the bridge inertia force at each time point can be obtained using the following steps: First, the acceleration for each element (or node) on the bridge model can be obtained directly after running the numerical program BIRDS-BVI; then, the inertia force of each element (or node) on the bridge model can be calculated as a product of the mass and acceleration of the element (or node). The effect of the inertia force of each element (or node) on the bridge response can then be obtained using influence surface concept; and finally, the effects of all elements (or nodes) on the bridge can be added to obtain the total effect of the total bridge inertia force on the response. An influence surface (a combination of all influence lines) for the bridge deflection at S5 is shown in Figure 5, where X represents the longitudinal direction of the bridge, Y represents the lateral direction, and Z is the deflection at S5 under a unit load moving across the bridge deck. Figure 5 was obtained with the ANSYS program.

Figure 6 shows the identified results for the interaction force with and without considering the bridge inertia force using the deflection and strain information, respectively. It can be easily seen from the Figure that neglecting the effect of the bridge inertia force could introduce significant errors in the identified results. However, in current weigh-in-motion methodology the inertia effect is either simply ignored or a low driving speed and/or smooth
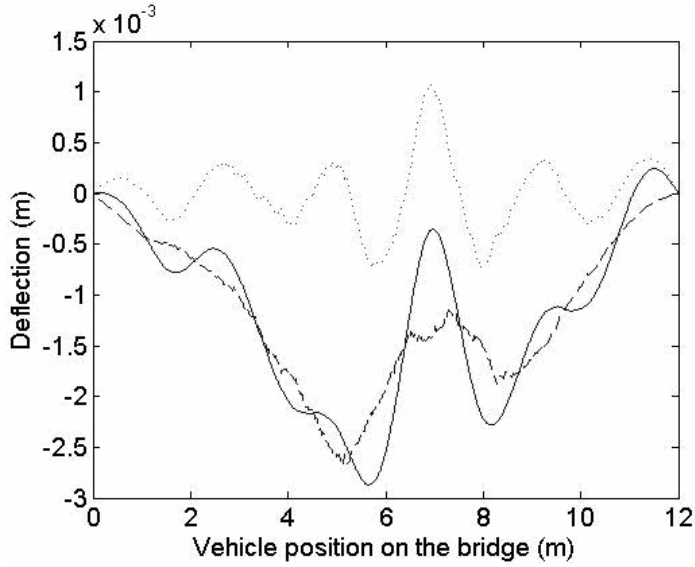
(a)
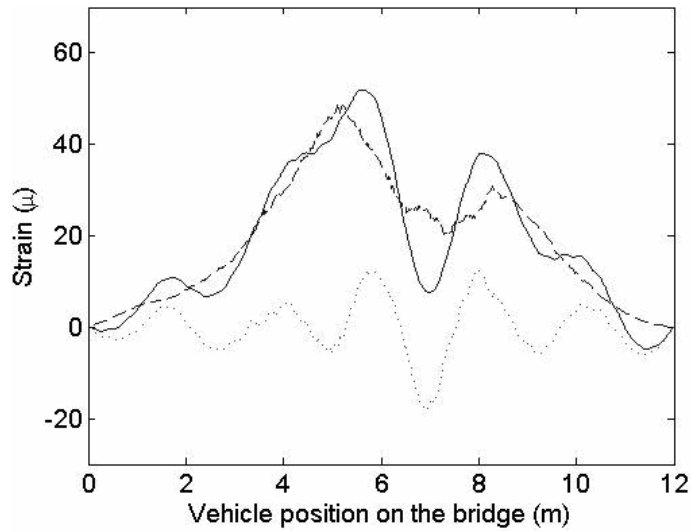
(b)

Figure 4. Decomposition of (a) deflection and (b) strain (—, total deflection (strain); – – –, deflection (strain) due to interaction force; · · · ·, deflection (strain) due to bridge inertia force).
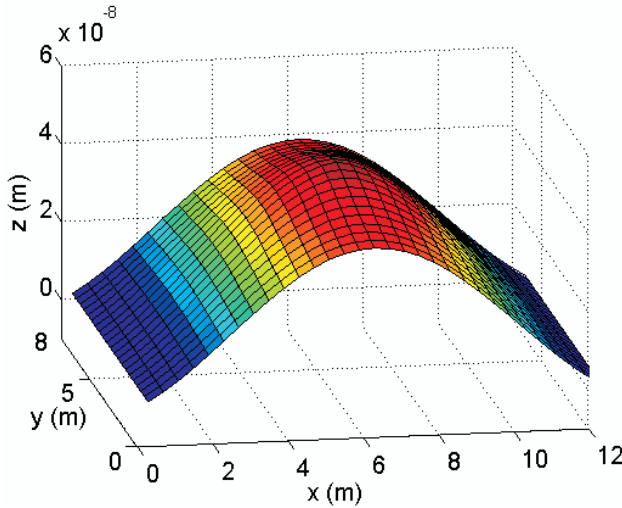
Figure 5. An influence surface for the deflection at S5.

surface is specified to reduce the dynamic effect. The same Figure also shows that using the deflection information can give better identification results than that obtained by using the strain information.

Although using the deflection information can give better results, some discrepancy does exist between the true axle loads and the identified results, mainly at the moments when the vehicle enters and leaves the bridge, especially for the identification results using the strain information. This phenomenon was reported by other researchers (Chan and Ashebo, 2006; Pinkaew, 2006). One possible reason for this is that the values on the influence surface, both for the deflection and strain, at both ends of the bridge are very small values resulting in sensitive results. Another possible reason could be that the strain obtained at a certain point from the developed program is only an approximate value, as can be seen from equation (22). However, we can exclude these invalid data points at bridge ends and obtain statistic axle load information for the structural design using the more reliable data when vehicles are closer to the mid-span.

4.2. Effect of Different Measurement Station

To study the sensitivity of identified results to measurement stations, the identification results using the deflection and strain information from the four different measurement stations when the vehicle is traveling along R2 are shown in Figure 7. As can be seen from Table 2, using information from S5 produces the best results while using information from S1 produces the worst ones. Also, information from S4 and S5, which are both located at the center line of the bridge, give better results than S1 and S2, both of which are not located at the center line of the bridge.
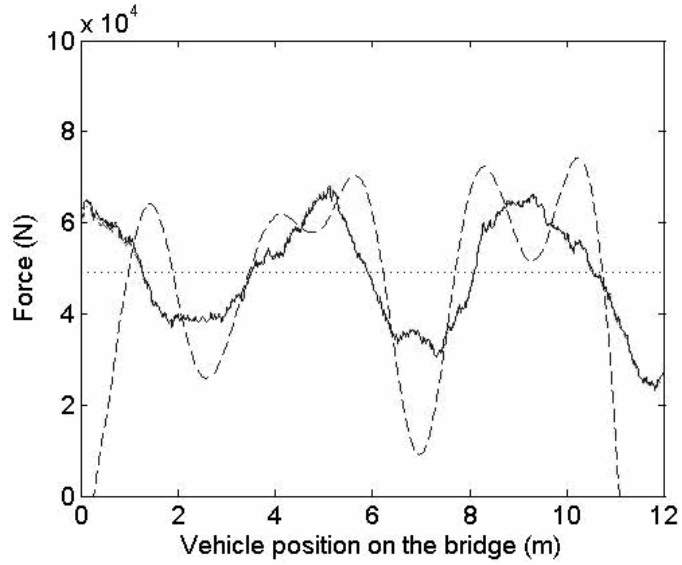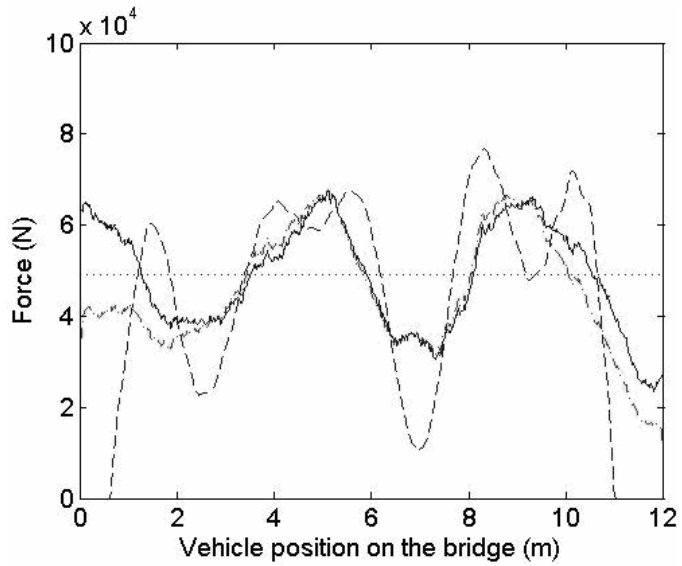
Figure 6. Identified force using (a) deflection, (b) strain (—, true force; · · · ·, static force; – · – · –, considering bridge inertia force; – – –, without considering bridge inertia force).
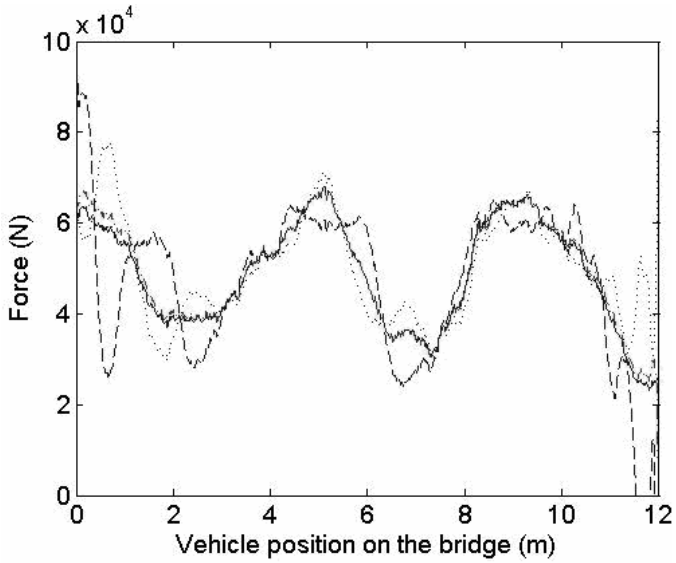
(a)
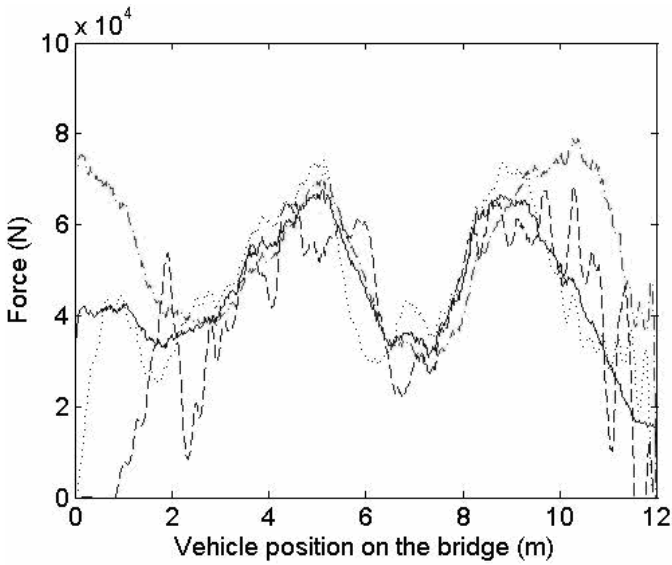
(b)

Figure 7. Identified forces from different measurement stations (a) using deflection, (b) using strain (—, S5; − · − · −, S4; · · · ·, S2; − − −, S1).

4.3. Effect of Different Vehicle Speeds

To examine whether vehicle traveling speeds would affect the accuracy of identifications, three levels of vehicle speeds were studied in this study: 5 m/s, 10 m/s, and 20 m/s. In all three cases, the vehicle is traveling along R2 with a constant speed. The deflection and strain information from S5 were used in the identification process. The identified results are shown in Figure 8. As can be seen from this Figure and Table 2, the vehicle speed almost has no effect on the accuracy of the identified results, indicating that the developed methodology can be used for routine traffic conditions. In comparison, most weigh-in-motion facilities do not work well for normal traveling vehicles and are only reliable for slow traffic (Ansari, 1990; Pinkaew, 2006).

4.4. Effect of Different Traveling Route

Vehicles can travel on a bridge in different lanes. In this study three cases in which a vehicle traveled along three different routes (R1 = width/8, R2 = width/4, and R3 = width/2 as indicated in Figure 2) were studied. The results in Figure 9 and Table 2 show that the accuracy of the identified results is not affected by the route along which the vehicle is traveling on the bridge, which, again, indicates the applicability of the developed methodology for actual, routine traffic conditions.

4.5. Effect of Number of Vehicles

Usually, more than one vehicle is traveling on a bridge at the same time. To verify the proposed method for this situation, two case studies were carried out. In the first case, the two vehicles traveled along the same route (R1), with one traveling in front of the other at a distance of 4 m. In the second case, the two vehicles traveled along two different routes (R1 and R4), with one traveling in front of the other at a distance of 4 m in the longitudinal direction.

   To identify the interaction forces from the two vehicles, response information from two measurement stations is needed, as discussed earlier. In this study S4 and S5 were used, and the identified results are shown in Figures 10 and 11 for the two cases, respectively. The results in these Figures and in Table 2 show that the addition of the second vehicle introduces more errors than the case of one-vehicle only, and larger errors occur at the moments when the second vehicle is entering the bridge and the first vehicle is leaving the bridge, which was also observed by Chan and Ashebo (2006). However, as discussed earlier, since in practice the two ends of the time history of the identified forces are not of interest and can be excluded, the error of the identified results could be reduced significantly.

4.6. Effect of Different Road Surface Condition

Three levels of different road surface conditions were studied, namely good, average, and poor, according to ISO 1995. The identified results using information from S5 are shown in Figure 12. As can be seen from the figure and Table 2, though the magnitude of the true interaction force becomes larger as the road surface condition gets worse, the accuracy
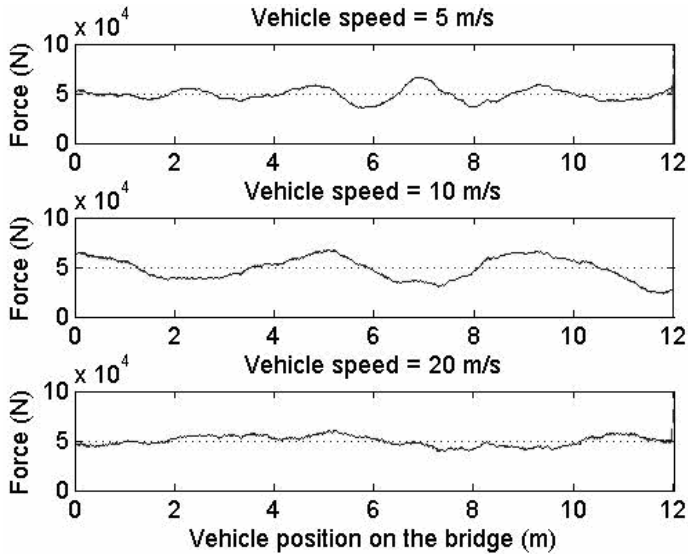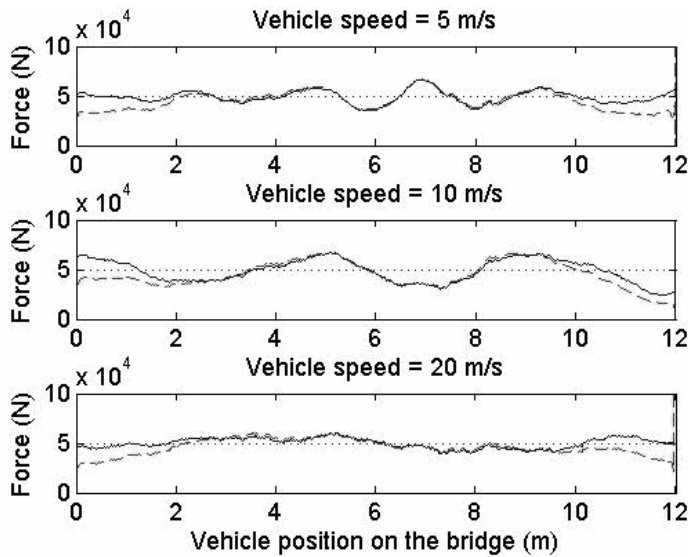
Figure 8. Identified forces for different vehicle speeds (a) using deflection, (b) using strain (——, true force; – · – · –, identified force; · · · ·, static force).
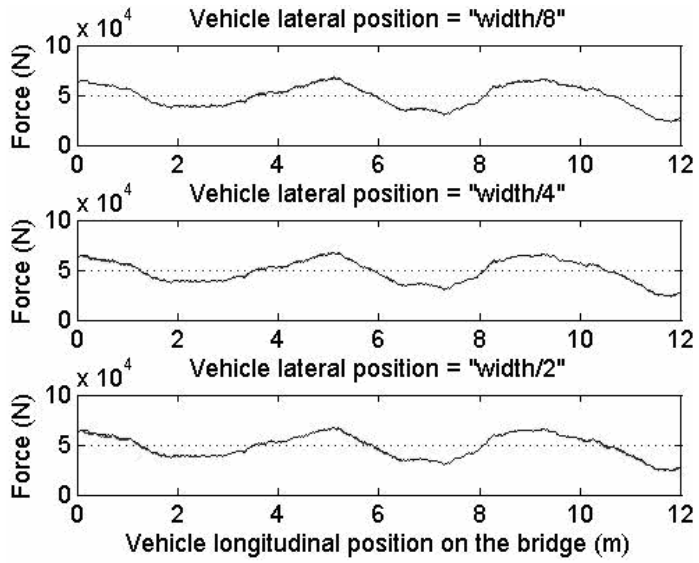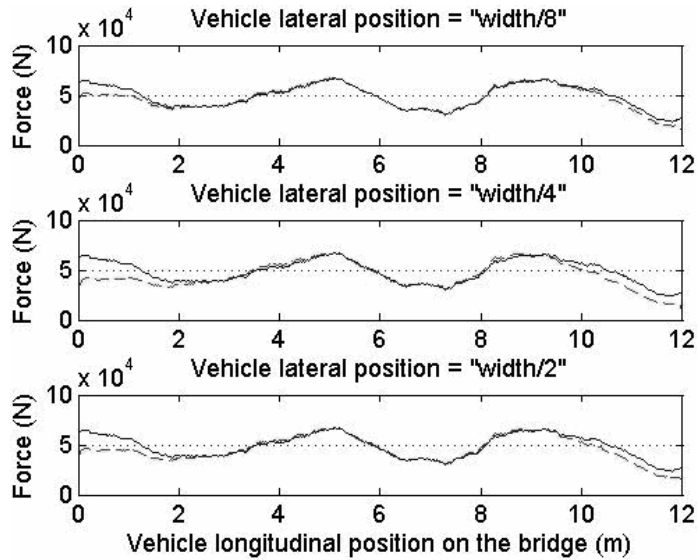
Figure 9. Identified forces for different traveling routes (a) using deflection, (b) using strain (—, true force; – · – · –, identified force; · · · ·, static force).
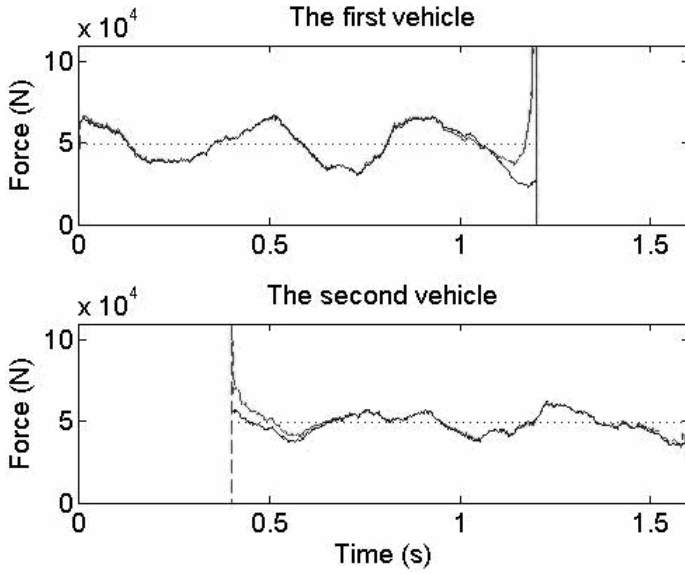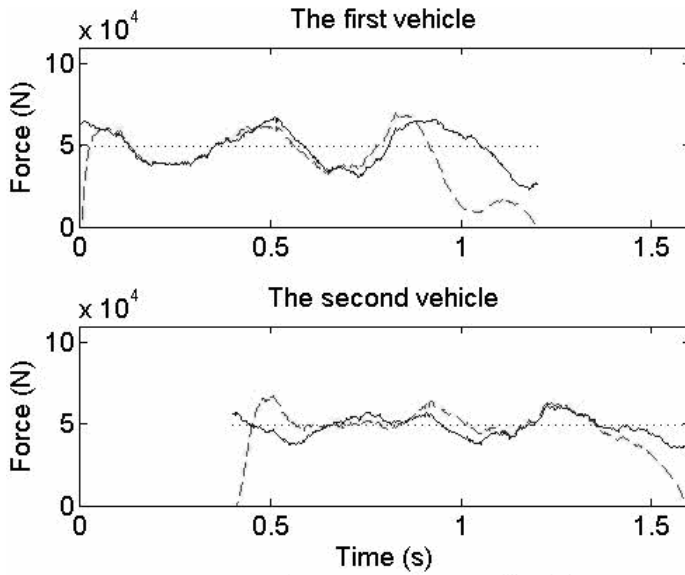
Figure 10. Identified forces for two vehicles traveling one in front of the other (a) using deflection, (b) using strain (—, true force; – · – · –, identified force; · · · ·, static force).
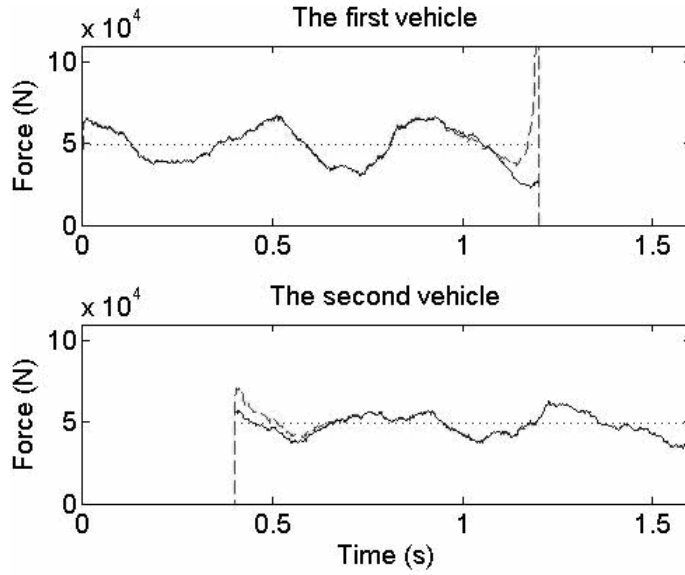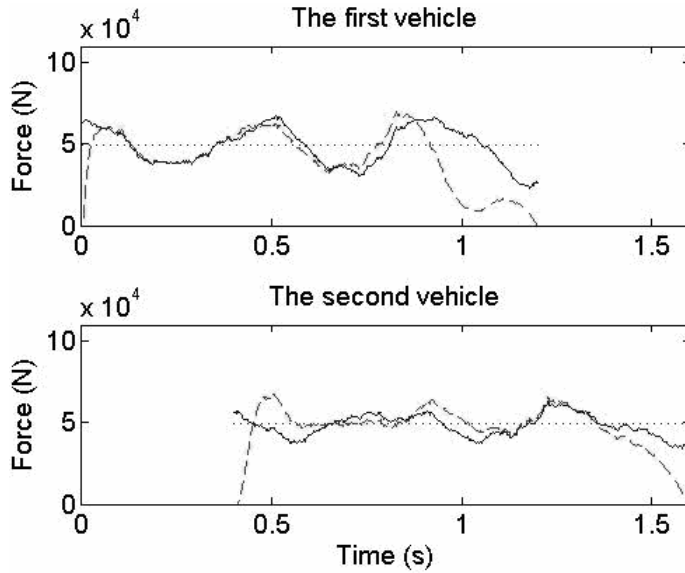
Figure 11. Identified forces for two vehicles traveling in different lane, one in front of the other (a) using deflection, (b) using strain (—, true force; – · – · –, identified force; · · · ·, static force).
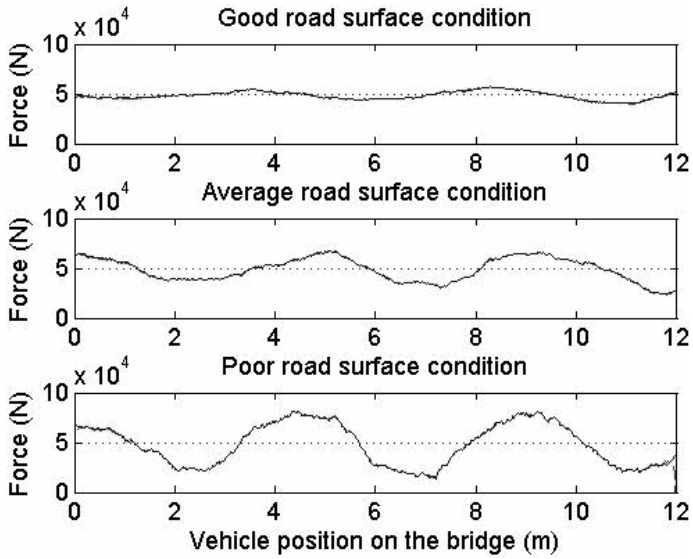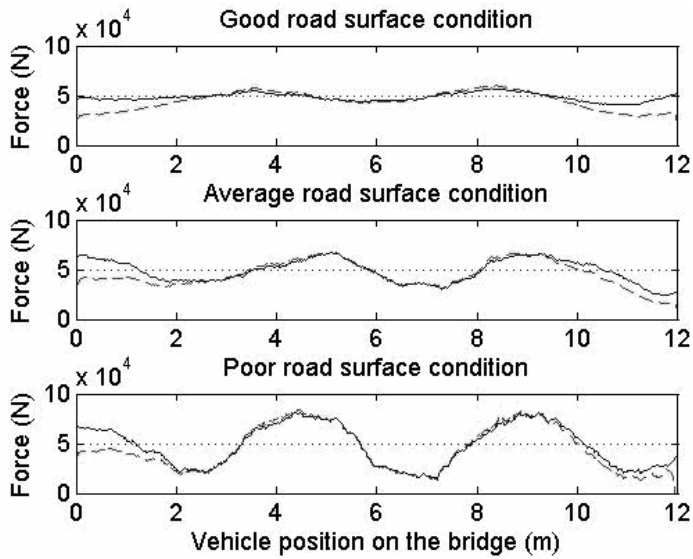
Figure 12. Identified forces under different road surface conditions (a) using deflection, (b) using strain
(—, true force; – · – · –, identified force; · · · ·, static force).
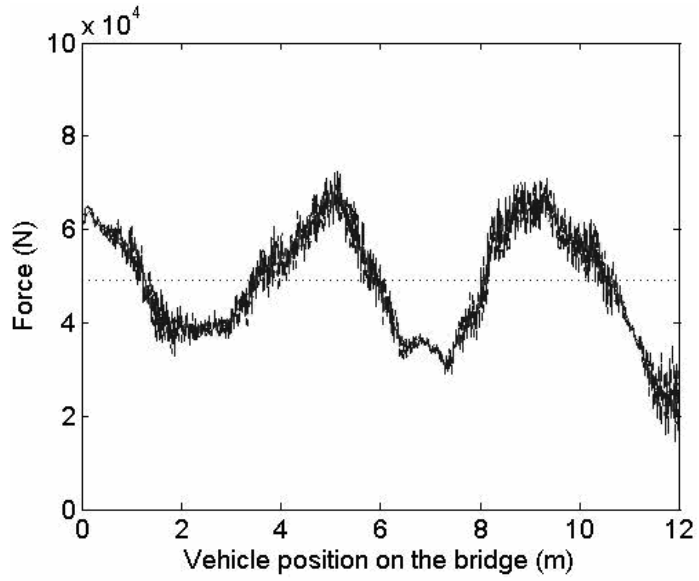
(a)
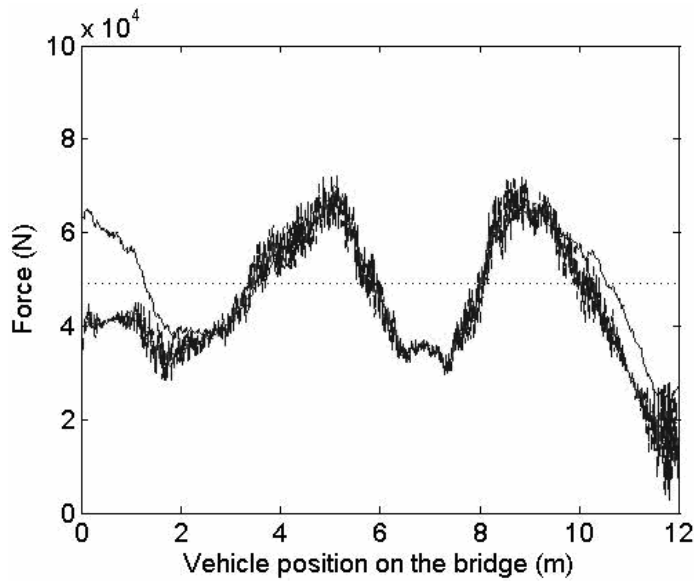
(b)

Figure 13. Identified force for different noise level (a) using deflection, (b) using strain (—, true force; — · — · —, 5% noise; – – –, 10% noise).

of the identification results is not affected. This occurs because the roughness-dependent inertia forces have been considered in the developed identification methodology. Again, most weigh-in-motion facilities do not work well with a rough surface condition which results in significant dynamic effects.

4.7. Effect of Different Noise Level

Since measurement noise always exists in real tests, the effect of measurement noise namely 5% and 10% was investigated in this numerical simulation. The identification results for the two levels of noise are shown in Figure 13. From the results we can easily observe that as the level of noise increase from 5% to 10%, the oscillation magnitude of the identification results around the non-noise curve increases. As shown in Table 2, the errors of identification for these two levels of noise are in a 3% to 5% range, respectively, if deflection is used. Larger errors exist when strain is used for identification.

5. CONCLUSIONS

A new method of identifying the time-varying axle loads using bridge responses is proposed. The proposed method employs the superposition principle and the concept of influence surface in the identification process. To demonstrate the concept using numerical simulations, a vehicle-bridge coupled system is first established and a MATLAB program is developed to solve the vehicle-bridge coupled equations. Bridge and vehicle responses as well as the interaction forces between the bridge and vehicles can be generated from this program. Based on the results from a comprehensive case study, the following conclusions can be drawn:

(1) By neglecting the effect of the bridge inertia force, in this specific example, a significant error can be introduced in the axle load identification process.

(2) Using deflection information can generally give better results than using strain information because of the possible fact that the strain at one point obtained from the numerical program is only an approximate value near that point, and can therefore introduce relatively larger error.

(3) Factors such as vehicle speed, road surface condition, and route have an insignificant effect on the accuracy of the identified results. The error in the identified results increases with the increase of measurement noise.

(4) The selection of position for measurement stations has a significant impact on the identified results. The selection of measurement stations at the center of the bridge and near the mid-span usually gives the best results.

(5) Relatively large errors mainly occur at the moments when vehicles enter and leave the bridge where the values on the influence surface are small. This may also explain why the average errors in the case where two vehicles are present on the bridge at the same time are larger than those of the one-vehicle case. However, the results identified when trucks are near the bridge end can be excluded, and the rest of the data can be utilized to derive axle load information for structural designs.

(6) The accuracy of the proposed identification methodology depends on the accuracy of the influence surface. Therefore, in actual field applications, a reliable bridge model should be obtained through model updating based on field measurements.

(7) The proposed methodology may help improve the current bridge-weigh-in-motion techniques that usually require a smooth road surface and slow vehicle movement.

The developed methodology will also be useful in identifying real vehicle dynamic forces on bridges, which will provide more reliable live load information for site-specific bridge fatigue assessment and performance evaluation.

REFERENCES

American Association of State Highway and Transportation Officials (AASHTO), 2002, *Standard Specifications for Highway Bridges,* Washington, DC.

American Association of State Highway and Transportation Officials (AASHTO), 2004, *LRFD Bridge Design Specifications,* Washington, DC.

Ansari, S. A., 1990, "Investigation of improved accuracy limits for dynamic bridge weigh-in-motion system," M.Sc. thesis, Department of Civil Engineering, University of Maryland, College Park, MD.

Bilello, L. A., Bergman, L. A., and Kuchma, D., 2004, "Experimental investigation of a small-scale bridge model under a moving mass," *Journal of Structural Engineering* **130(5)**, 799–804.

Cebon, D., 1987, "Assessment of the dynamic wheel forces generated by heavy road vehicles," in *Proceedings of the Symposium on Heavy Vehicle Suspension and Characteristics*, *Australian Road Research Board*, Canberra, March 23–25.

Chan, T. H. T., Law, S. S., Yung, T. H., and Yuan, X. R., 1999, "An interpretive method for moving force identification," *Journal of Sound and Vibration* **219(3)**, 503–524.

Chan, T. H. T., Yu, L., and Law, S. S., 2000, "Comparative studies on moving force identification from bridge strains in laboratory," *Journal of Sound and Vibration* **235(1)**, 87–104.

Chan, T. H. T. and Ashebo, D. B., 2006, "Theoretical study of moving force identification on continuous bridges," *Journal of Sound and Vibration* **295,** 870–883.

Chatterjee, P. K., Datta, T. K., and Surana, C. S., 1994, "Vibration of suspension bridges under vehicular movement," *Journal of Structural Engineering* **120(3)**, 681–703.

Deng, L. and Cai, C. S., 2008, "Identification of dynamic vehicular axle loads: Demonstration by field study," *Journal of Vibration and Control* (submitted).

Dodds, C. J. and Robson, J. D., 1973, "The description of road surface roughness," *Journal of Sound and Vibration* **31(2),** 175–183.

Green, M. F. and Cebon, D., 1994, "Dynamic response of highway bridges to heavy vehicle loads: theory and experimental validation," *Journal of Sound and Vibration* **170**, 51–78.

Henchi, K., Fafard, M., Talbot, M., and Dhatt, G., 1998, "An efficient algorithm for dynamic analysis of bridges under moving vehicles using a coupled modal and physical components approach," *Journal of Sound and Vibration* **212**, 663–683.

Heywood, R. J., 1996, "Influence of truck suspensions on the dynamic response of a short span bridge over Cameron's Creek," *Heavy Vehicle Systems* **3(1–4)**, 222–239.

Huang, D. Z. and Wang, T. L., 1992, "Impact analysis of cable-stayed bridges," *Computers & Structures* **43(5)**, 897–908.

International Organization for Standardization (ISO), 1995, "Mechanical vibration-road surface profiles-reporting of measured data," ISO 8068: 1995 (E), ISO, Geneva.

Law S. S., Chan, T. H. T., and Zeng, Q. H., 1997, "Moving force identification: a time domains method," *Journal of Sound and Vibration* **201(1)**, 1–22.

Law, S. S., Chan, T. H. T., and Zeng, Q. H., 1999, "Moving force identification: A frequency and time domains analysis," *Journal of Dynamic Systems, Measurement, and Control* **12(3)**, 394–401.

Law S. S., Chan, T. H. T., Zhu, X. Q., and Zeng, Q. H., 2001, "Regularization in moving force identification," *Journal of Engineering Mechanics* **127(2)**, 136–148.

Law, S. S., Bu, J. Q., Zhu, X. Q., and Chan, S. L., 2007, "Moving load identification on a simply supported orthotropic plate," *International Journal of Mechanical Science* **49**, 1262–1275.

Leming, S. K. and Stalford, H. L., 2002, "Bridge weigh-in-motion system development using static truck/bridge model," in *Proceedings of the American Control Conference*, Anchorage, AK, pp. 3672–3677, May 8–10.

O'Conner, C. and Chan, T. H. T., 1988, "Dynamic wheel loads from bridge strains," *Journal of Structural Engineering* **114(8)**, 1703–1723.

Peters, R. J., 1984, "A system to obtain vehicle axle weights," in *Proceedings of the Twelfth Australian Road Research Board (ARRB) Conference*, Hobart, Australia, v12, pp. 19–29, Aug. 27–31.

Pinkaew, T., 2006, "Identification of vehicle axle loads from bridge responses using updated static component techniques," *Engineering Structure*s **28**, 1599–1608.

Pinkaew, T. and Asnachinda, P., 2007, "Experimental study on the identification of dynamic axle loads of moving vehicles from the bending moments of bridges," *Engineering Structures* **29**, 2282–2293.

Shi, X. M., 2006, "Structural performance of approach slab and its effect on vehicle induced bridge dynamic response," Ph.D. dissertation, Louisiana State University, Baton Rouge, LA.

Shi, X. M., Cai, C. S., and Chen, S. R., 2008, "Vehicle induced dynamic behavior of short span bridges considering effect of approach span condition," *ASCE, Journal of Bridge Engineering* **13(1)**, 83–92.

Tikhonov, A. N., 1963, "On the solution of ill-posed problems and the method of regularization," *Soviet Mathematics* **4**, 1035–1038.

Yang, B., Tan, C. A., and Bergman, L. A., 2000, "Direct numerical procedure for solution of moving oscillator problems," *Journal of Engineering Mechanics* **126(5)**, 462–469.

Yang, Y. B. and Yau, J. D., 1997, "Vehicle-bridge interaction element for dynamic analysis," *Journal of Structural Engineering* **123,** 1512–1518.

Yu, L. and Chan, T. H. T., 2003, "Moving force identification based on the frequency-time domain method," *Journal of Sound and Vibration* **261(2)**, 329–349.

Yu, L. and Chan, T. H. T., 2007, "Recent research on identification of moving loads on bridges," *Journal of Sound and Vibration* **305**, 3–21.

Zhang, Y., Cai, C. S., Shi, X. M. and Wang, C., 2006, "Vehicle induced dynamic performance of a FRP versus concrete slab bridge," *ASCE, Journal of Bridge Engineering* **11(4)**, 410–419.

Zhu, X. Q. and Law, S. S., 2002, "Practical aspects in moving load identification," *Journal of Sound and Vibration* **258(1),** 123–146.

Zhu, X. Q. and Law, S. S., 2003, "Dynamic axle and wheel loads identification: Laboratory studies," *Journal of Sound and Vibration* **268**, 855–879.